Electronic Supplementary Material (ESI) for Nanoscale.

Supporting Information. Wettability-defined droplet imbibition in ceramic mesopores

Adnan Khalil[1], Felix Schäfer[1], Niels Postulka[1], Mathias Stanzel[1], Markus Biesalski[1], Annette Andrieu-Brunsen[1]*

[1]Ernst-Berl-Institut für Technische und Makromolekulare Chemie, Technische Universität Darmstadt, 64287 Darmstadt, Germany

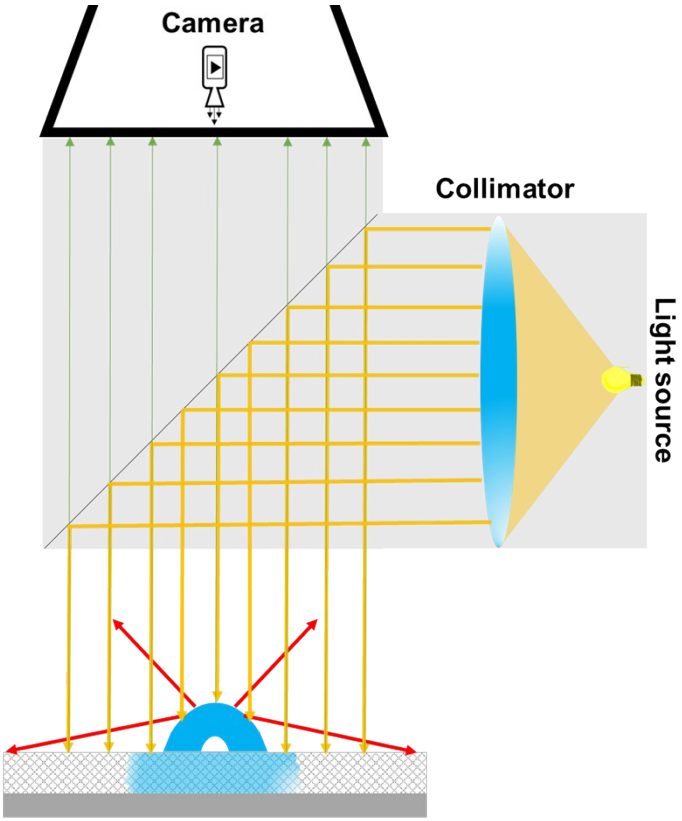

Figure S1. Schematic image of the collimated coaxial illumination used for the observation and recording of water imbibition in mesoporous silica thin films.

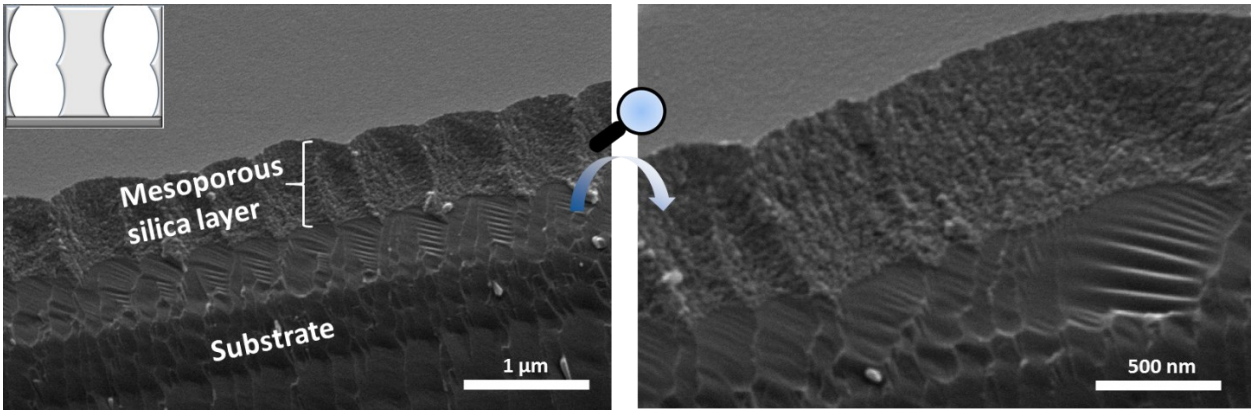

Figure S2. Cross-section SEM image of the applied mesoporous silica thin films. SEM and ellipsometry coincide regarding the film thickness (500 – 600 nm).

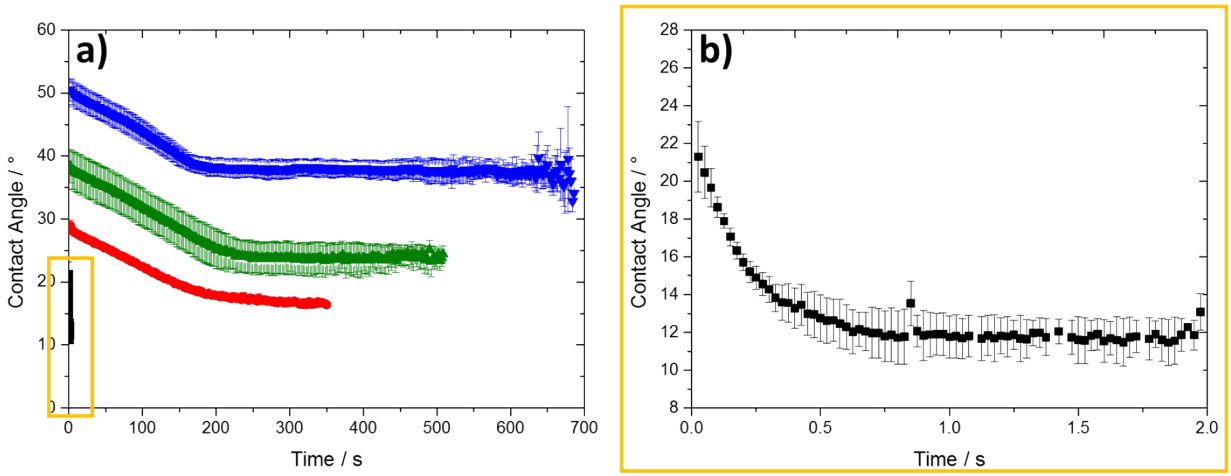

Figure S3. Contact angle measurements corresponding to the top view imbibition videos (a) as well as a zoom-in for the reference (b). If possible the whole process from droplet deposition to evaporation was recorded and evaluated (black: reference, CA ~ 20°, red: CA ~ 30°, green: CA ~ 40°, blue: CA ~ 50°, scale bar = 2 mm).

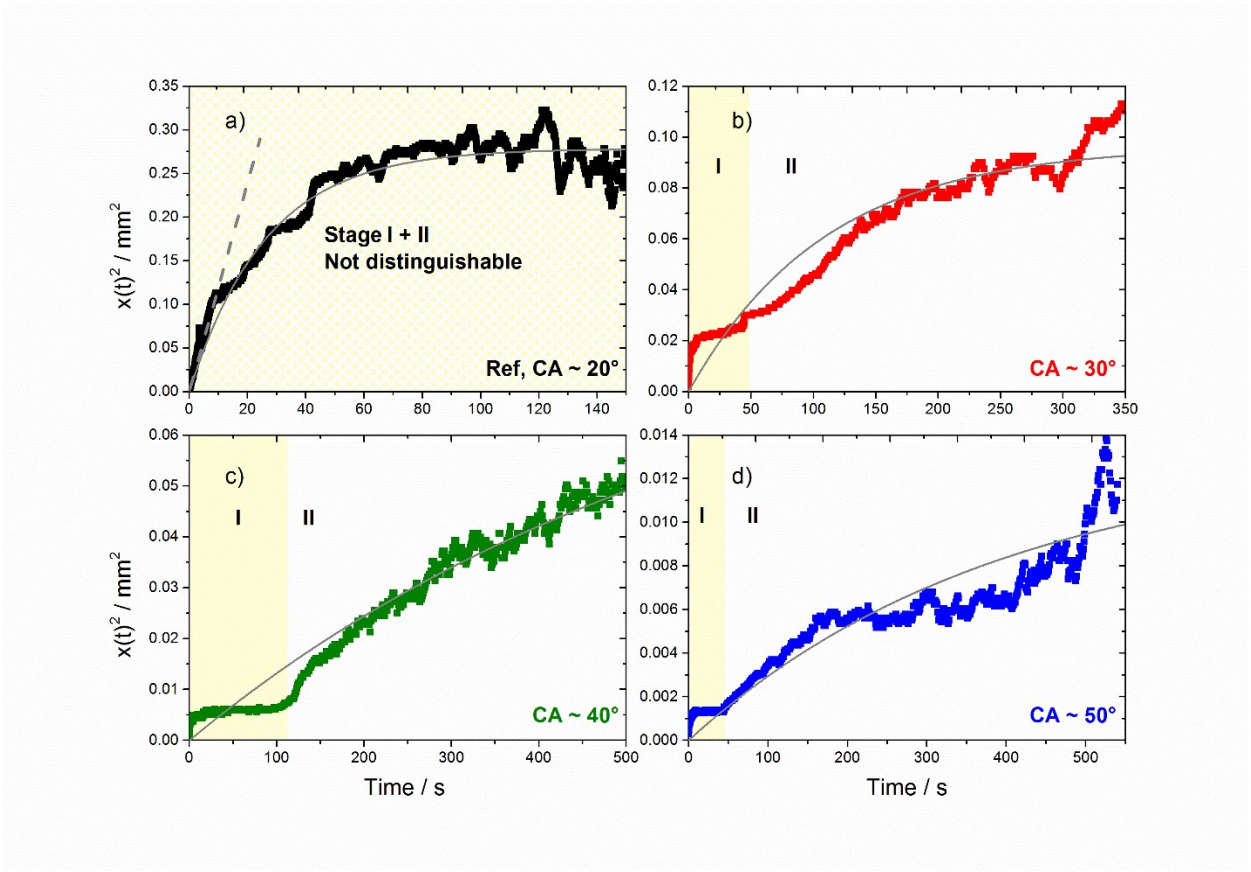

Figure S4. Squared imbibition data of water in mesoporous silica thin films before and after functionalization: a) black: Reference, CA ~ 20°, b) red: CA ~ 30°, c) green: CA ~ 40°, d) blue: CA ~ 50°. In all curves the grey line corresponds to the fit using equation (1). The dotted grey line in a) indicates an initial linear increase. The yellow-shaded area marks the first stage of imbibition, apparently following the modified Lucas-Washburn law.

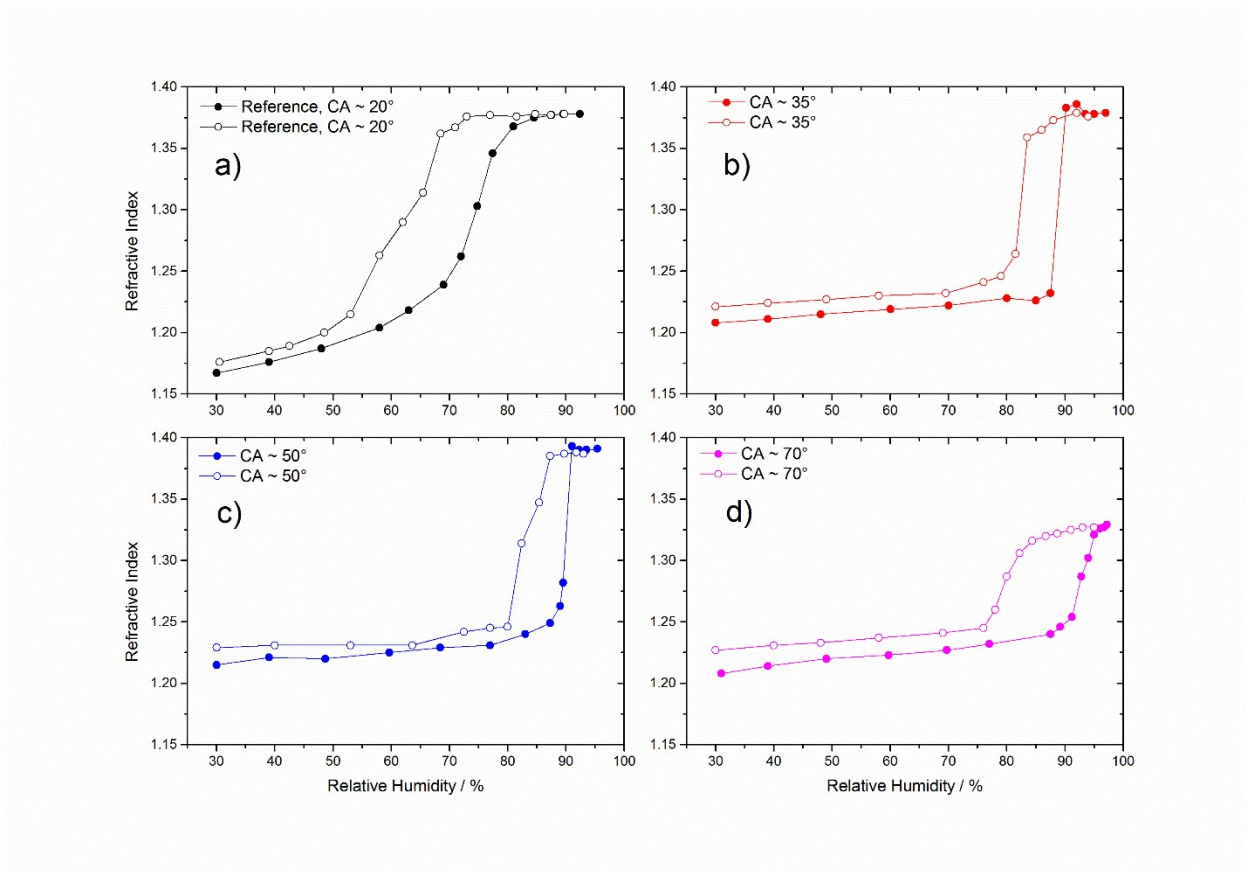

Figure S5. Influence of the CA on the sorption behavior of water as reflected by the refractive index in dependence of increasing relative humidities for a) a mesoporous reference, b) a mesoporous silica thin film with a CA of ~ 35°, c) a mesoporous silica thin film with a static CA of ~ 50° and d) a mesoporous silica thin film with a static CA of ~ 70°.

Prior to the actual sorption measurements the films were wetted and dewetted by exposing the samples to a gradual in-/ and decrease of RH in several steps as also described in the experimental section:

1: Wetting: RH ~30% → RH ~45% → RH ~75% → RH ≥ 90%

2: Dewetting: RH ≥ 90% → RH ~75% → RH ~45% → RH ~ 30%

3: Sorption measurement depicted in Figure S5

When comparing the four different refractive indices (n), of an unfunctionalized reference sample as well as a functionalized sample (CA ~ 35°) at a relative humidity of ~30%, the values reveal that the hysteresis does not close after the pre-treatment but rather increases (Table S1).

Table S1. Comparison of refractive index (n), of an unfunctionalized reference sample as well as a functionalized sample (CA ~ 35°), at a relative humidity of ~30% during a pre-treatment (ads/des, pretreatment) and during a subsequent complete sorption measurement (ads/des).

Sample	**Relative Humidity** / %	**n (ads, pre-treatment)**	**n (des, pre-treatment)**	**n (ads)**	**n (des)**
Reference (before functionalization)	~30	1.164	1.167	1.167	1.176
35° (after functionalization)	~30	1.200	1.208	1.208	1.221

Expemplary calculation of nanoscopic contact angle at capillary condensation:

The nanoscopic contact angle was calculated by rearranging the Kelvin-equation. For the calculation an exemplary pore radius of 3.7 nm was used.

Rearranged Kelvin-equation:

$$\theta = cos^{-1}\left(\frac{-ln\frac{p_c}{p_0}rRT}{2\gamma V_m}\right)$$

Rearranged Kelvin-equation considering strongly adsorbed water film:[1-2]

$$\theta = cos^{-1}\left(\frac{-ln\frac{p_c}{p_0}(r-t)RT}{2\gamma V_m}\right)$$

(p_c/p_0 = relative pressure at capillary condensation (0.75 / 0.87 / 0.9 / 0.93), V_m = molar volume [$18.07*10^{-6}$ m^3/mol], r = pore radius [$3.7*10^{-9}$ m], t = thickness of water adsorption layer [$0.4*10^{-9}$ m], γ = surface tension [$72.75*10^{-3}$ kg/s^2], R = gas constant [8.314 kgm^2/s^2molK,] T = temperature [293.15 K] θ = contact angle)

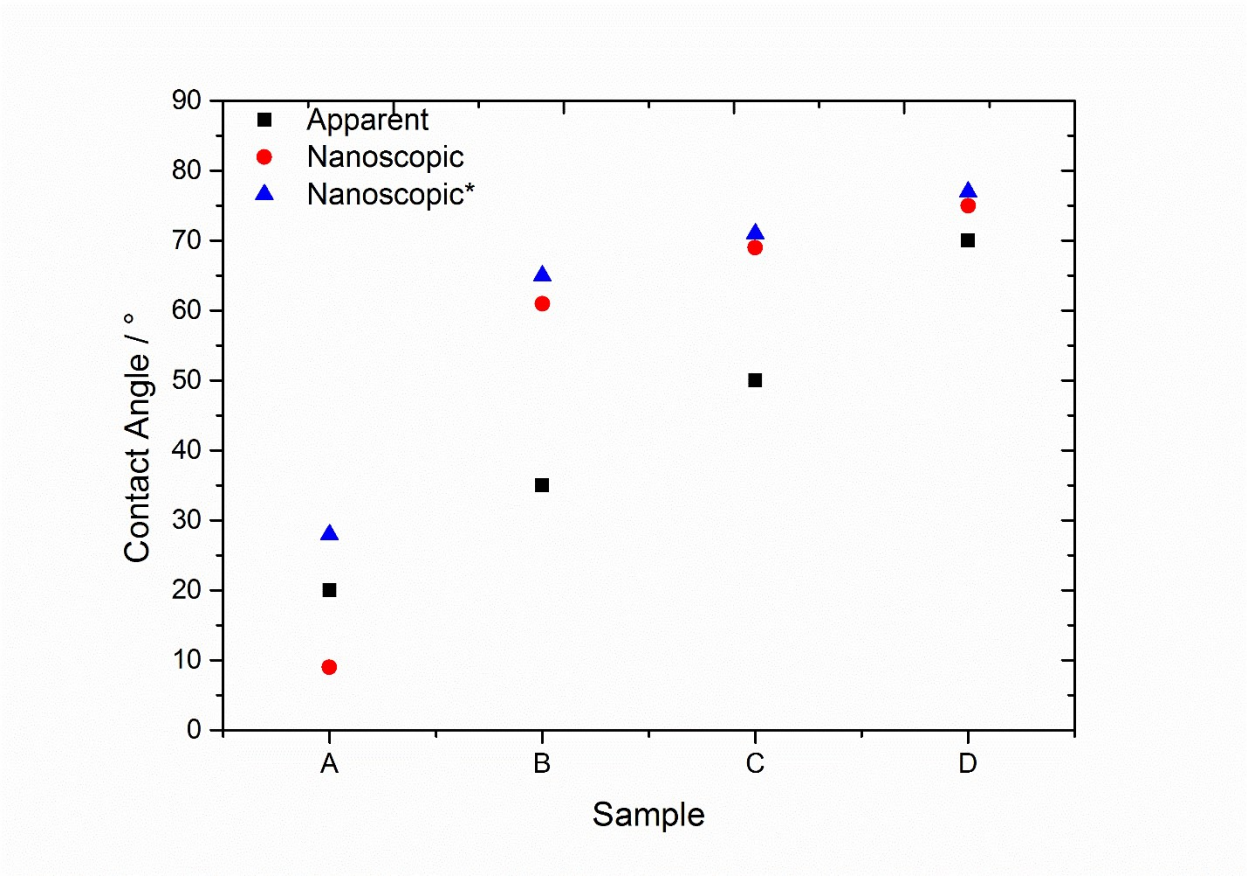

Figure S6. Calculated nanoscopic contact angle, with (*) and without consideration of a strongly adsorbed water layer (thickness t = 0.4 nm)[3-5] on the silica surface, in comparison to measured apparent contact angle. For the calculation the relative pressure data of **Figure S5** was used.

Role of mesoporous structure on capillary condensation:

When observing the sorption of a gas in a mesoporous network the material of the matrix, the pore size, pore shape, pore volume, roughness of the pore walls as well as the shape of the adsorbing molecules have to be considered. This is well described in the IUPAC technical report by Thommes et al. (Pure Appl. Chem. 2015; 87(9-10): 1051–1069). The physorption in mesopores initiates with a monolayer adsorption so that all the adsorbed molecules are in direct contact with

the surface of the mesoporous matrix. Afterwards more layer of molecules are added on top of the monolayer (multilayer formation) until a critical vapor pressure is reached and liquid bridges form due to capillary condensation. With the addition of more molecules, the menisci move forward to the pore ends until the pore space is completely filled (J. Phys.: Condens. Matter 2015; 27 103102). The capillary condensation is typical for meso-sized pores and occurs at a pressure p that is lower than the saturation pressure of the bulk liquid (p^0). In case of even smaller micropores the term capillary condensation is not appropriate since it does not involve a vapor-liquid transition.

According to the 1985 IUPAC recommendation (Pure Appl. Chem. 1985; 27) as well as the updated technical report (Pure Appl. Chem. 2015; 87(9-10): 1051–1069) mesoporous materials show a Type IV isotherm. Depending on the morphology of the mesoporous system the capillary condensation can be accompanied by a hysteresis (Type IV a) or not (Type IV b). Thereby, network effects as well as pore blocking define the desorption. Narrow pore necks hinder the emptying of wider pores, therefore the desorption begins at lower vapor pressures than the critical vapor pressure (which causes capillary condensation). Therefore elliptical mesopores (as applied in this study) rather show a hysteretic sorption behavior than cylindrical mesopores, which have more uniform porous structure and pore diameter. For a more detailed description of this phenomenon the reader is referred to the extensive work of Ceratti et al. (Nanoscale 2015; 7; 5371-5382).

The hysteresis loop itself can be divided even further into different classifications, again depending on the porous morphology. Typically, templated silica which exhibit a narrow range of uniform mesopores show a Type H1 hysteretic loop (Pure Appl. Chem. 2015; 87(9-10): 1051–1069), which is a defined by a steep adsorption as well as steep desorption branch. For more complex porous e.g. if the size distribution of pore necks widths is larger, structures network effects and pore blocking become more important and e.g. cause a broadening of the hysteretic loop. The

mesoporous thin films used in this work (**Figure S5**) exhibit a Type IV isotherm and a mixture of a Type H1 and Type H2 b hysteretic loop, which is typical for templated silica materials with pore diameters > 4 nm. Upon functionalization the isotherm seems to change into a Type V isotherm, which can be typical for water adsorption on hydrophobic mesoporous adsorbents (Pure Appl. Chem. 2015; 87(9-10): 1051–1069). This was also addressed in a previous publication of our group (J. Coll. Int. Sci. 2020; 560: 369-378).

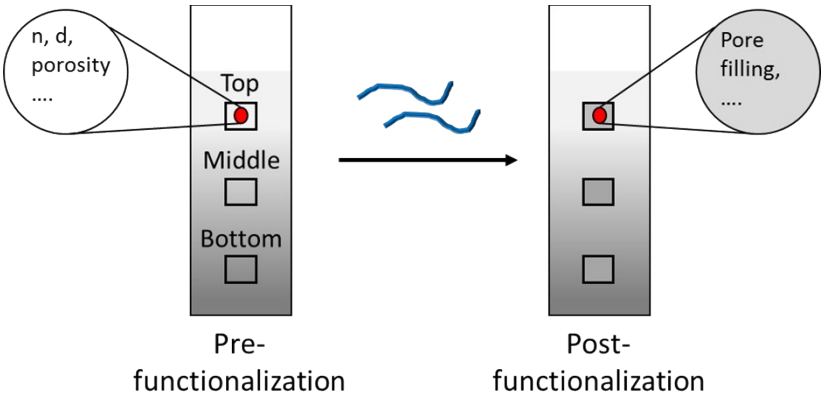

Figure S7. Schematic view of samples for ellipsometry measurements. Before the first measurements and prior to functionalization the samples are marked at three positions, at the top, the middle and the bottom, respectively. The ellipsometry measurements are executed at this marked positions. The obtained data regarding the refractive index (n) and the layer thickness (d) are compared for each position before and after functionalization, delivering information about porosity and pore filling.

Table S2. Refractive index (n), layer thickness determined by ellipsometry before (white table) and after different amount of functionalization (grey table), leading to different contact angles (CA) and pore filling.

Pre-functionalization			**Post-functionalization**		
Position	d / nm	n	d / nm	n	Resulting CA and pore filling

Top Middle Bottom	536.6 ± 3.7 603.1 ± 6.4 601.3 ± 6.5	1.141 ± 0.003 1.156 ± 0.005 1.173 ± 0.006	544.6 ± 4.5 587.8 ± 6.3 585.6 ± 6.2	1.170 ± 0.004 1.195 ± 0.006 1.214 ± 0.006	CA ~ 35° 16 %
Top Middle Bottom	499.4 ± 3.2 531.9 ± 3.5 556.7 ± 4.3	1.158 ± 0.003 1.156 ± 0.003 1.161 ± 0.004	501.7 ± 3.2 526.6 ± 4.0 537.8 ± 4.3	1.192 ± 0.003 1.199 ± 0.004 1.219 ± 0.005	CA ~ 50° 20 %
Top Middle Bottom	494.4 ± 3.6 540.3 ± 3.7 555.0 ± 4.4	1.152 ± 0.003 1.151 ± 0.003 1.154 ± 0.004	489.2 ± 2.7 532.8 ± 4.3 533.5 ± 4.4	1.192 ± 0.003 1.211 ± 0.005 1.216 ± 0.004	CA ~ 70° 23 %
Top Middle Bottom	511.1 ± 3.3 561.6 ± 4.3 561.8 ± 4.5	1.149 ± 0.003 1.150 ± 0.004 1.151 ± 0.004	480.4 ± 2.6 536.7 ± 4.4 537.5 ± 4.3	1.190 ± 0.003 1.224 ± 0.005 1.217 ± 0.005	CA ~ 80° 26 %

Table S3. Refractive index (n), layer thickness determined by ellipsometry before (white table) and after incubation in water (grey table). The initial Young's CA of the sample was ~ 50°.

Before water incubation			**After water incubation**	
Position	d / nm	n	d / nm	n
Top Middle Bottom	546.8 ± 3.4 570.9 ± 4.8 575.7 ± 5.0	1.164 ± 0.003 1.187 ± 0.005 1.196 ± 0.005	550.1 ± 3.7 568.9 ± 4.6 575.1 ± 5.0	1.166 ± 0.003 1.188 ± 0.005 1.199 ± 0.005

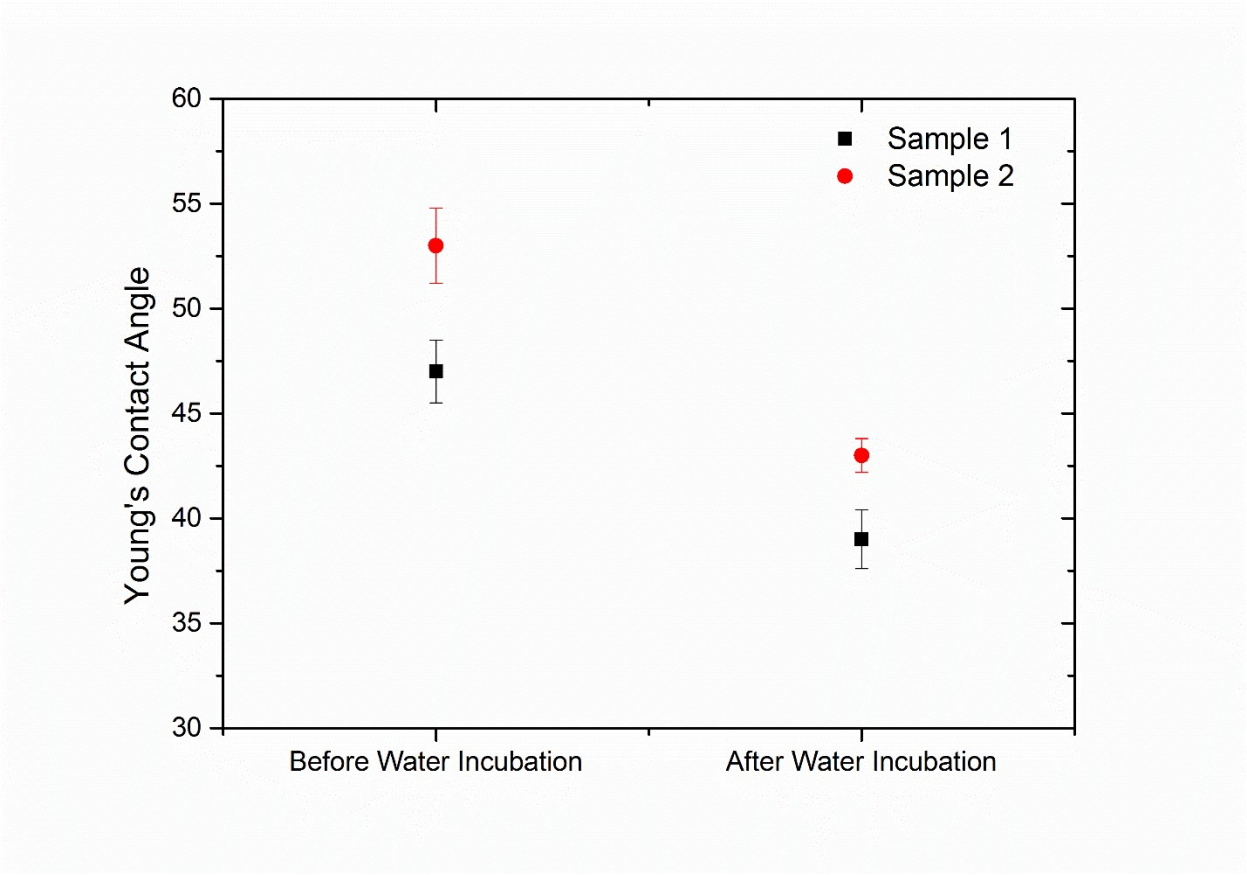

Figure S8. Young's CA of two different mesoporous silica thin films (functionalized with PFODMCS) before and after water incubation in water.

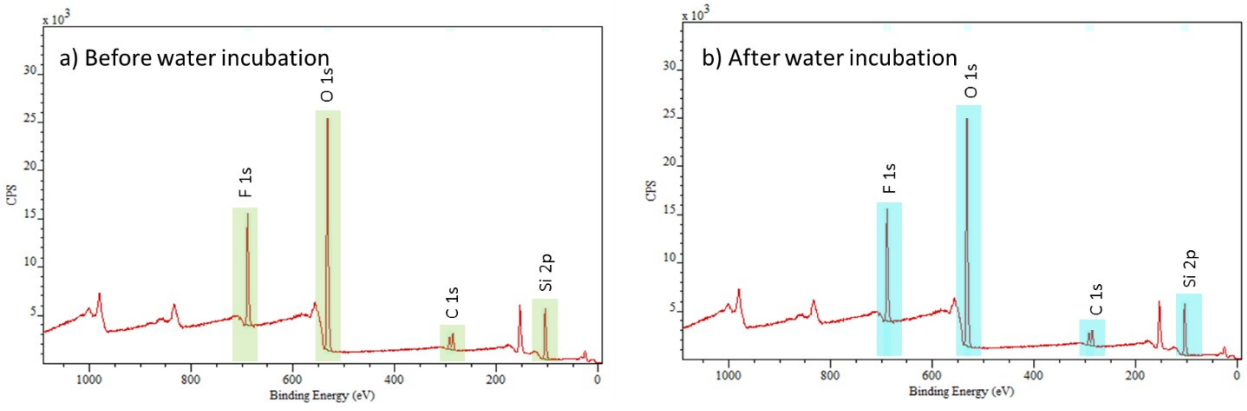

Figure S9. Binding spectra of XPS-measurements for functionalized mesoporous silica thin film (CA ~ 50°) before (a) after water incubation (b).

Table S 4. ESCA element-concentration were determined by XPS-Measurements before and after water incubation of a functionalized mesoporous silica thin film (CA ~ 50°).

Sample	C/ at%	O/ at%	Si/ at%	F/ at%	F/Si - ratio
Before water incubation	12	47	25	16	0.6
After water incubation	12	48	25	15	0.6

1. Kruk, M.; Jaroniec, M.; Sayari, A., Application of large pore MCM-41 molecular sieves to improve pore size analysis using nitrogen adsorption measurements. *Langmuir* **1997,** *13* (23), 6267-6273.
2. Van Honschoten, J. W.; Brunets, N.; Tas, N. R., Capillarity at the nanoscale. *Chemical society reviews* **2010,** *39* (3), 1096-1114.
3. Schreiber, A.; Ketelsen, I.; Findenegg, G. H., Melting and freezing of water in ordered mesoporous silica materials. *Physical Chemistry Chemical Physics* **2001,** *3* (7), 1185-1195.
4. Asay, D. B.; Kim, S. H., Evolution of the adsorbed water layer structure on silicon oxide at room temperature. *The Journal of Physical Chemistry B* **2005,** *109* (35), 16760-16763.
5. Xiao, C.; Shi, P.; Yan, W.; Chen, L.; Qian, L.; Kim, S. H., Thickness and structure of adsorbed water layer and effects on adhesion and friction at nanoasperity contact. *Colloids and Interfaces* **2019,** *3* (3), 55.